

Article

# One-Pot Synthesized Pd@N-Doped Graphene: An Efficient Catalyst for Suzuki–Miyaura Couplings

Mufsir Kuniyil <sup>1</sup>, J. V. Shanmukha Kumar <sup>1,\*</sup>, Syed Farooq Adil <sup>2,\*</sup>,  
Mohammed Rafi Shaik <sup>2</sup>, Mujeeb Khan <sup>2</sup>, Mohamed E. Assal <sup>2</sup>,  
Mohammed Rafiq H. Siddiqui <sup>2</sup> and Abdulrahman Al-Warthan <sup>2</sup>

<sup>1</sup> Department of Chemistry, Koneru Lakshmaiah Education Foundation, Vaddeswaram, Guntur 522502, Andhra Pradesh, India; mufsir@gmail.com

<sup>2</sup> Department of Chemistry, College of Science, King Saud University, P.O. Box 2455, Riyadh 11451, Saudi Arabia; rafiskm@gmail.com (M.R.S.); kmujeeb@ksu.edu.sa (M.K.); mhd.elshahat@gmail.com (M.E.A.); rafiqs@ksu.edu.sa (M.R.H.S.); awarthan@ksu.edu.sa (A.A.-W.)

\* Correspondence: shanmukh\_fed@kluniversity.in (J.V.S.K.); sfadil@ksu.edu.sa (S.F.A.); Tel.: +966-11-467-0439 (S.F.A.)

Received: 14 April 2019; Accepted: 7 May 2019; Published: 21 May 2019



**Abstract:** Nitrogen-doped graphene (NDG)-palladium (Pd)-based nanocatalysts (NDG@Pd) can be potentially applied as an efficient catalyst for the preparation of biaryls in a Suzuki–Miyaura coupling reaction. Herein, we report the one-pot facile synthesis of an NDG@Pd nanocatalyst, wherein the nanocatalyst was prepared by the simultaneous reduction of graphene oxide (GRO) and PdCl<sub>2</sub> in the presence of hydrazine hydrate as a reducing agent, while ammonium hydroxide was used as a source of “N” on the surface of graphene. The as-synthesized NDG@Pd nanocatalyst, consisting of smaller-sized, spherical-shaped palladium nanoparticles (Pd-NPs) on the surface of NDG, was characterized by several spectroscopic and microscopic techniques, including high-resolution transmission electron microscopy (HRTEM), X-ray diffraction (XRD), ultraviolet–visible spectroscopy (UV-Vis), Fourier-transform infrared spectroscopy (FT-IR), X-ray photoelectron spectroscopy (XPS), and Brunauer–Emmett–Teller (BET). The nanocatalyst displayed outstanding catalytic activity in the Suzuki–Miyaura cross-coupling reactions of phenyl halides with phenyl boronic acids under facile conditions in water. The catalytic activity of NDG@Pd was found to be a more efficient catalyst when compared to pristine highly reduced graphene oxide (HRG) based Pd nanocatalyst (HRG@Pd). Furthermore, the reusability of the catalyst was also tested by repeatedly performing the same reaction using the recovered catalyst. The N-doped catalyst displayed excellent reusability even after several reactions.

**Keywords:** palladium nanoparticles; N-doped graphene; nanocatalyst; Suzuki–Miyaura coupling; catalytic activity

## 1. Introduction

Graphene is a carbon allotrope in which an atomically thin layer of sp<sup>2</sup> hybridized carbon atoms are densely packed, i.e., in a honeycomb crystal lattice [1,2]. This specifically “2D” material displays exclusive electronic qualities and high crystal properties and is considered to be novel material for a variety of exciting applications, including catalysis [3–5]. The physicochemical properties of graphene can be further improved by the inclusion of several functional components, such as polymers, biomolecules, and inorganic nanoparticles such as metal and metal oxide nanoparticles [6]. The combinations of graphene and various transition metals such as Pd, Pt, Au, etc., provide extraordinary strength and value to the resulting composite material, which may exhibit exceptional

performance in several advanced applications ranging from the medical to the energy sector, including catalysis [7,8]. In this regard, highly reduced graphene oxide (HRG) not only exhibits the potential to be a promising catalyst, but also to function as an attractive support material in a variety of hybrid catalysts. Particularly, the catalytic activities of HRG-based materials can be increased either by doping with various heteroatoms or blending them with other inorganic nanomaterials to form functional nanocomposites. Among inorganic nanomaterials, graphene based Pd nanocomposites have offered exciting results in a variety of catalytic applications in several organic transformations. The coordinated effects and inherent properties of both HRG and Pd, such as the large surface area of HRG, the ample presence of active sites, and the unique catalytic performance of Pd, collectively enhance the catalytic properties of the resulting hybrid nanocatalyst. Therefore, graphene-based palladium nanocomposites have been largely applied in a variety of catalytic applications.

So far, these types of catalysts have been applied in several industrially important organic transformations, such as oxidations, reductions, hydrogenations, and activations of the C–H bond etc. [9]. Among these transformations, cross-coupling reactions such as Heck, Kumada, Stille, Sonogashira, and Suzuki–Miyaura have attained enormous attention in numerous fields [10–12]. Particularly, the Suzuki–Miyaura reaction is the most important type of coupling reaction and has been extensively applied in the formation of C–C bonds between an organo-boron compound and an organic (pseudo) halide in the presence of transition metals as catalysts [13,14]. In this regard, Pd has been the most versatile catalyst for the formation of C–C bonds, particularly for Suzuki–Miyaura-type cross-coupling reactions [15,16]. Particularly, due to the high surface area and other exciting surface properties of graphene, Pd-based HRG nanocomposites have attained significant attention as a catalyst in this type of reaction [17]. As a support, the HRG in the nanocatalyst provides a huge boost to the surface area of the catalyst, which considerably enhances the interaction between the substrate and the catalyst [18].

Generally, during the preparation, HRG-Pd nanocomposites suffer from an aggregation of nanoparticles (NPs), resulting in a low density and non-uniform coverage of NPs on the surface of graphene, due to which their catalytic applications are seriously affected. Chemical modification of an inactive graphene surface is typically performed to achieve homogeneous dispersion of NPs on the surface of graphene. However, in many cases, the chemical functionalization adversely affects various properties of graphene, including surface area and electrical conductivity [19]. In this scenario, nitrogen doping (N-doping) provides an excellent alternative for the dispersion of metal NPs on the surface of graphene without causing significant damage to the properties of the resulting material [20,21]. The excess of nitrogen on the surface of graphene considerably influences the growth mechanism of NPs, which not only helps in controlling the size and shape of the NPs, but also facilitates the uniform dispersion of NPs [22]. Besides, N-doping also provides stability to the resulting composite, as it offers potential binding sites during the dispersion of NPs on the surface of HRG [23]. During doping, some of the carbon atoms on the surface of the graphene may get substituted with nitrogen atoms, which disturbs the conjugation and aromaticity of the graphene and causes the formation of additional defective sites. Furthermore, high electronegativity of nitrogen also causes the formation of catalytic active sites, due to which nitrogen-doped graphene-based materials have also been used as metal-free electrocatalytic catalysts [24–27]. Therefore, N-doped palladium-based nanocomposites possess huge potential and can be effectively applied in Suzuki cross-coupling reactions [28].

Herein, we report the one-pot synthesis of nitrogen-doped graphene (NDG)-palladium (Pd) nanocatalysts (NDG@Pd), in which graphene oxide (GRO) synthesized using the Hummers method, was simultaneously reduced along with PdCl<sub>2</sub> using hydrazine hydrate as a reducing agent and ammonium hydroxide as a source of nitrogen on the surface of highly reduced graphene oxide. The synthesized NDG@Pd was characterized by several spectroscopic and microscopic procedures, including high-resolution transmission electron microscopy (HRTEM), X-ray diffraction (XRD), ultraviolet–visible spectroscopy (UV-Vis), Fourier-transform infrared spectroscopy (FT-IR), X-ray photoelectron spectroscopy (XPS), and Brunauer–Emmett–Teller (BET). Finally, the as-synthesized

NDG@Pd nanocatalyst was applied to Suzuki–Miyaura cross-coupling reactions under aqueous circumstances and aerobic conditions. Moreover, the reusability of the resultant catalyst was also tested by performing various reactions using the recovered catalyst.

## 2. Results and Discussions

### 2.1. UV Analysis

To begin with, a nitrogen-doped graphene-palladium nanocatalyst was prepared by the simultaneous reduction of both GRO and a palladium precursor in the presence of ammonium hydroxide as a doping agent. The as-prepared nanocatalyst was used as a catalyst in a Suzuki–Miyaura coupling reaction. In order to study the effect of nitrogen doping on the catalytic activity of the resultant nanocatalyst, the catalytic activity of the NDG@Pd was compared to HRG@Pd, which was prepared in the absence of a doping agent. Initially, the formation of both of the nanocatalysts was confirmed using UV-spectroscopy. Figure 1 displays the absorbance spectra of the GRO (pink line), PdCl<sub>2</sub> (Red line), NDG@Pd (green line), and HRG@Pd (blue line) nanocatalysts. The reduction of GRO was confirmed by the absence of the characteristic absorption peaks of GRO in both HRG@Pd and NDG@Pd, which typically appear in GRO at ~230 and ~300 nm [29]. Similarly, PdCl<sub>2</sub> exhibited a typical absorption peak at ~415 nm, which also disappeared after the reduction and formation of Pd nanoparticles. Therefore, the absence of the peaks of both GRO and PdCl<sub>2</sub> in both NDG@Pd and HRG@Pd clearly pointed toward the formation of nanocatalysts. In comparison, the UV spectrum of NDG@HRG exhibited a small absorption peak at ~275 nm, which was attributed to the presence of an excess of nitrogen on the surface of HRG and appeared due to the electronic transition between carbon and nitrogen atoms [30].

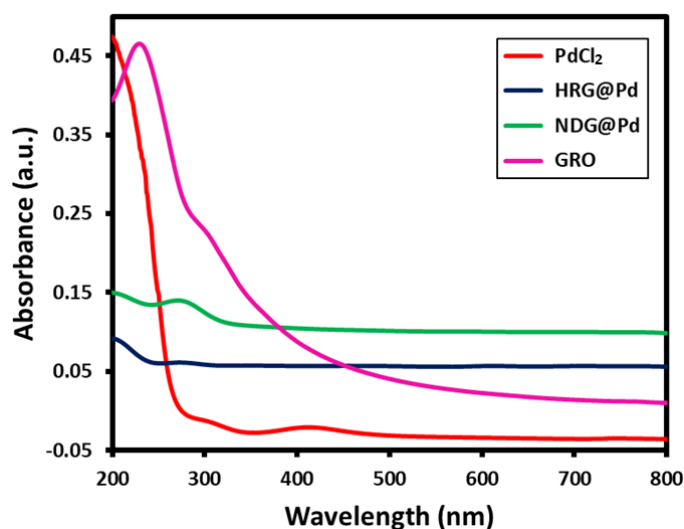


**Figure 1.** UV-Vis absorption spectra of palladium chloride (red line), graphene oxide (GRO) (pink line), the highly reduced graphene-based palladium nanocatalysts (HRG@Pd) (blue line), and the nitrogen-doped graphene-based palladium nanocatalyst (NDG@Pd) (green line).

### 2.2. FT-IR Analysis

Figure 2 exhibits the FT-IR spectra of GRO, NDG@Pd, and HRG@Pd. The IR spectrum of GRO typically exhibited several bands, as shown in Figure 2 (pink line), which represent the oxygenated groups on the surface, such as hydroxyl, carboxyl, ester, and epoxy groups. Due to different modes, such as bending or stretching, these groups contributed to various prominent peaks in the spectrum, which occurred at ~3415, ~2920, ~2850, ~1850, ~1730, ~1627, and ~1050 cm<sup>-1</sup>, etc. After reduction, some of these peaks either disappeared or their intensities were reduced due to the removal of these groups, which was an indication of the successful reduction of GRO to HRG. This was clearly observed in the IR spectrum of HRG@Pd (Figure 2, blue line), in which the intensities of peaks belonging to the

OH group at  $\sim 3420\text{ cm}^{-1}$  and other peaks were considerably reduced. Similarly, the IR peaks in the spectrum of NDG@Pd were also reduced, pointing toward the successful reduction of GRO. Besides, the nitrogen doping in the sample of NDG@Pd was confirmed by the presence of two characteristic peaks at  $\sim 1325$  and  $\sim 1570\text{ cm}^{-1}$ , which were attributed to the stretching of the C–N bond from the secondary aromatic amine, which pointed toward bonding between carbon and nitrogen [31].

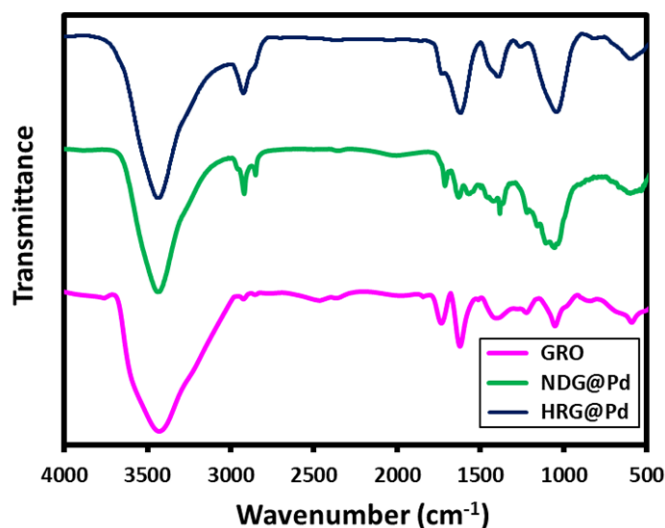


**Figure 2.** FT-IR spectra of graphene oxide (GRO) (pink line), highly reduced graphene-based palladium nanocatalysts (HRG@Pd) (blue line), and nitrogen-doped graphene-based palladium nanocatalyst (NDG@Pd) (green line).

### 2.3. XRD Analysis

The XRD diffraction pattern of GRO, NDG@Pd, and HRG@Pd are shown in Figure 3. GRO, upon the oxidation of pristine graphite, exhibited characteristic diffraction peaks at a lower Bragg angle of  $2\theta = 10.9^\circ$  due to the incorporation of oxygenated groups between the graphene layers. The reduction of GRO is commonly confirmed by the disappearance of this characteristic peak and by the emergence of a broad new peak at a slightly higher Bragg angle of  $2\theta = 22.4^\circ$ . In both NDG@Pd and HRG@Pd, the absence of a GRO peak at  $10.9^\circ$  and the appearance of a broad peak at  $\sim 22.4^\circ$  clearly confirmed the reduction of GRO. Besides, the XRD pattern of these samples also consisted of several other prominent reflections at a higher Bragg angle, which could be attributed to the Pd NPs. For instance, five distinct reflections in the diffractogram at  $40.02^\circ$  (111),  $46.49^\circ$  (200),  $68.05^\circ$  (220),  $81.74^\circ$  (311), and  $86.24^\circ$  (222) belonged to the face-centered cubic (fcc) structure of Pd NPs (JCPDS: 87-0641; space group: Fm3m (225)) [32]. This clearly confirmed the formation of nitrogen-doped graphene based Pd (NDG@Pd) and HRG@Pd nanocatalysts. Furthermore, in order to ascertain the phase changes in the catalyst upon use, the used catalyst was subjected to XRD analysis and the pattern obtained was compared to the pattern obtained using the freshly prepared catalyst (Figure S1). It was found that there is no significant change in the phase composition in the catalyst, NDG@Pd, upon use.

### 2.4. TEM Analysis of the NDG@Pd Nanocatalyst

Transmission electron microscopy (TEM) could be used to directly determine the nature and morphology of nanoparticles formed on the surface of graphene in the NDG@Pd nanocatalyst. The NDG@Pd nanocatalyst exhibited the crumpled sheet-like structure of the nitrogen-doped graphene (NDG) and spherically shaped Pd NPs on its surface, as shown in Figure 4. The NPs were largely homogeneously distributed on the surface of NDG, but in some places these particles were slightly aggregated and possessed an average diameter of 6.9 nm.

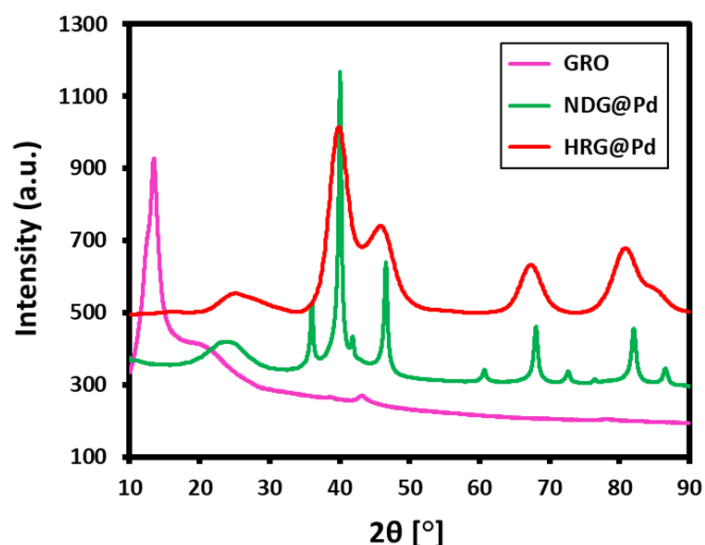


**Figure 3.** XRD diffractogram of graphene oxide (GRO) (pink line), highly reduced graphene-based palladium nanocatalyst (HRG@Pd) (red line), and nitrogen-doped graphene-based palladium nanocatalyst (NDG@Pd) (green line).

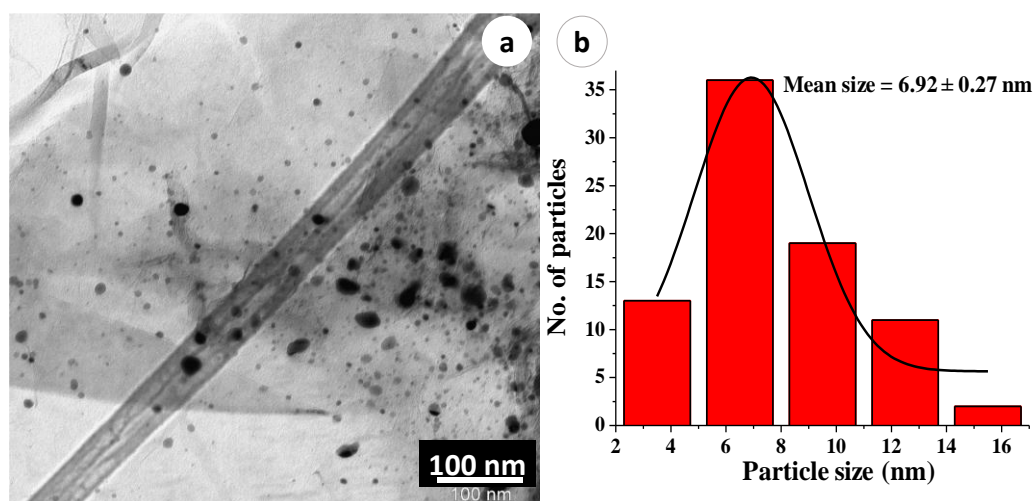


**Figure 4.** (a) High-resolution transmission electron microscope (TEM) images and (b) particle size distribution of the NDG@Pd nanocatalyst.

### 2.5. BET Analysis

Adsorption–desorption isotherms were studied employing BET and yielded Type IV isotherms, which were indicative of the mesoporous nature of the NDG@Pd. However, upon comparison to HRG@Pd, it was found that the mesoporous nature was retained upon doping with nitrogen and Pd (Figure 5). The specific surface area measurements of the samples demonstrated that HRG@Pd and NDG@Pd possessed a surface area of 461.19 and 355.39 m<sup>2</sup>/g, respectively. The high specific surface area of HRG@Pd was mainly attributed to the chemical reduction of GRO, which significantly reduced the number of oxygenated groups and water molecules from the surface and edges of graphene layers, which ultimately led to the expansion and exfoliation of graphene layers. However, the NDG@Pd exhibited a small specific surface area compared to HRG@Pd due to the doping with nitrogen atoms, which created more defects and distorted the surface of the material. The doped graphene samples typically had a smaller surface area when compared to undoped graphene due to the lesser degree of exfoliation induced by the reduction process, since the intercalation of doping atoms between graphene layers leads to the distortion of the layered structure, which has a negative influence on the surface

area of the material [33]. Pore size distribution curves were plotted for NDG@Pd nanocatalysts and showed that the pore size was found to be in the range of 25–45 nm, which was similar to the HRG@Pd. However, it was found that the pore volume of the HRG@Pd was slightly higher than that of the NDG@Pd nanocatalysts (Figure 6).

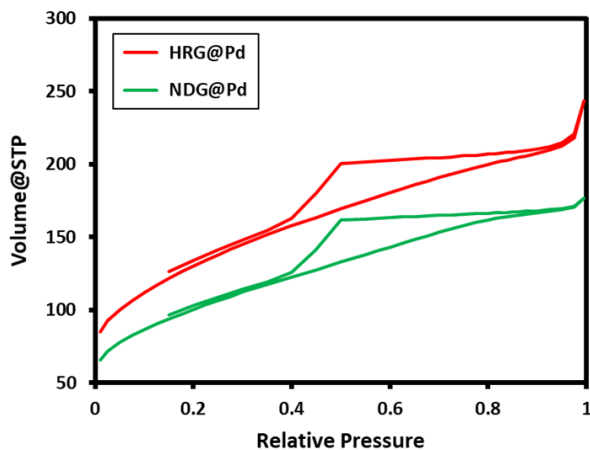


**Figure 5.** Adsorption–desorption isotherm of the highly reduced graphene-based palladium nanocatalyst (HRG@Pd) and the nitrogen-doped graphene-based palladium nanocatalyst (NDG@Pd).

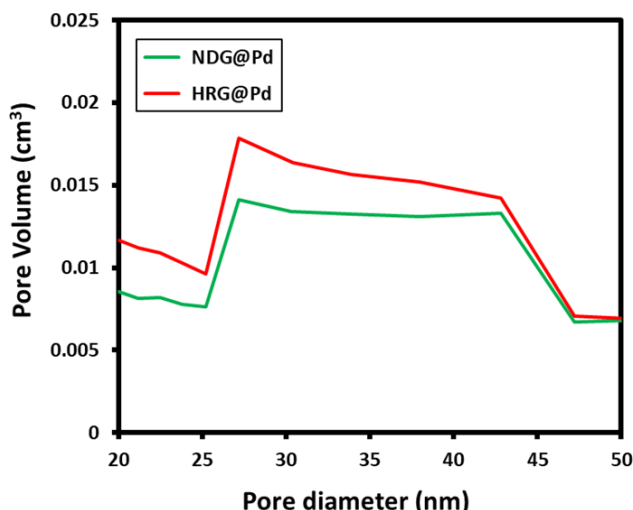


**Figure 6.** Pore size distribution of the highly reduced graphene-based palladium nanocatalyst (HRG@Pd) and the nitrogen-doped graphene-based palladium nanocatalyst (NDG@Pd).

## 2.6. XPS Analysis of the NDG@Pd Nanocatalyst

The use of XPS was employed to determine the existence of different forms of nitrogen species present on the surface of the graphene and the oxidation state of Pd present in the system. The XPS survey scan spectrum of NDG@Pd is given in Figure 7, demonstrating the presence of predominant C 1s, O 1s, N 1s, and Pd 3d peaks.

XPS analysis further revealed that the surface compositions of the palladium supported nitrogen-doped graphene oxide sheets. Notably, the C 1s line scan yielded peaks at 284.5 eV and 285 eV, which corresponded to graphite-like  $sp^2$ -hybridized carbon and an  $sp^2$  C=N bond, indicating the formation of a C–N bond on the surface of the graphene sheet [34,35]. The curve-resolved spectrum of N 1s yielded two peaks with a binding energy of 400 eV and 405 eV, which corresponded to the pyridinium and pyrrolic forms of nitrogen in the NDG@Pd [36]. Upon evaluation, it was found that the atomic percentage of both of the forms of nitrogen in the NDG@Pd were found to be in the ratio 1:1. The corresponding O 1s spectrum could be deconvoluted into four peaks with binding energies

of 529.6 eV, 531 eV, 533 eV, and 534.6 eV. The signal at 531 eV could be assigned to oxygen-bonded Pd (Pd–O), while 529.6 eV, 533 eV, and 534.6 eV could be attributed to the presence of –C=O, –C–OH, chemisorbed oxygen (carboxylic groups), and/or water, respectively [37,38]. The high-resolution XPS spectrum of the Pd 3d region (Figure 8) yielded peaks at binding energies of 335.1 eV, 335.8 eV, and 337.6 eV, which corresponded to  $3d_{5/2}$  and 340.3 eV, 341.1 eV, and 342.3 eV, which corresponded to  $3d_{3/2}$ . The XPS signals revealed the existence of Pd in the form of  $Pd^{2+}$  and  $Pd^0$ : The existence of  $Pd^{2+}$  could be attributed to the coordination Pd with oxygen moieties present on the surface of nitrogen-doped highly reduced graphene oxide, as confirmed by the O 1s spectrum. The third peak fit for the shoulder appearing at the base of Pd  $3d_{3/2}$  and Pd  $3d_{5/2}$  could be attributed to oxygen deficiency, which could have been due to the undercoordinated Pd sites of ultrasmall PdO nanoparticles [39]. The atomic percentage of Pd in the composite was found to be 20%, which was estimated by the area of C, O, and N peaks in the XPS spectrum.

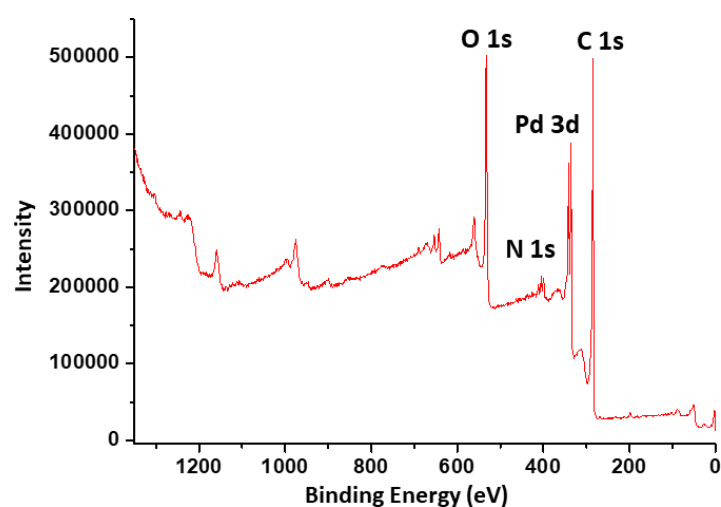


Figure 7. X-ray photoelectron spectroscopy (XPS) scan survey of NDG@Pd composites.

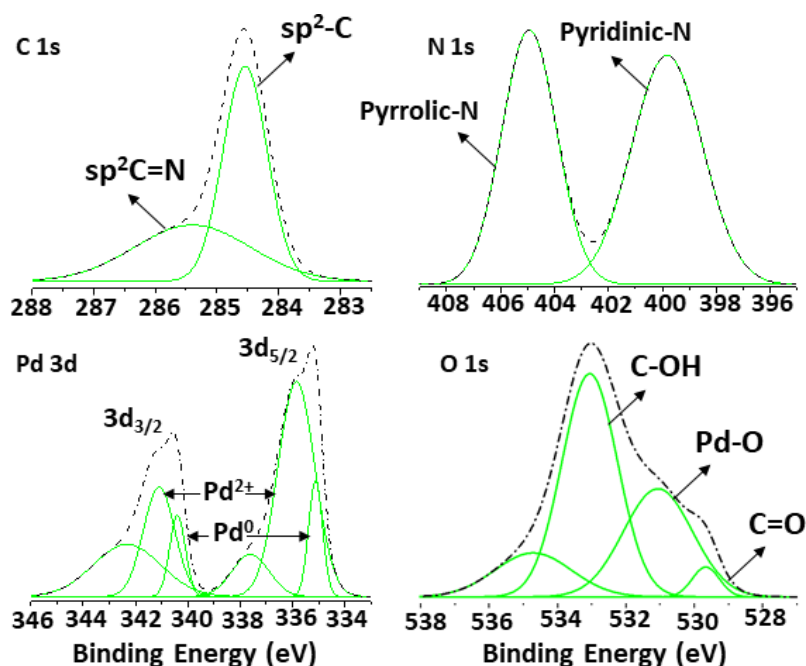


Figure 8. High-resolution XPS elemental scan of NDG@Pd composites.

### 2.7. Suzuki Reaction Catalyzed by NDG@Pd Nanocatalyst

In Suzuki coupling, nanopalladium-based heterogeneous catalysts have gained great success due to their smaller size and high surface area, resulting in enhanced contact between the substrate and the catalyst [40]. As-synthesized nitrogen-doped graphene-based palladium nanocatalyst was investigated in the Suzuki–Miyaura coupling of bromo-, chloro-, and iodobenzene with phenylboronic acid in aqueous medium [17]. In this circumstance, the synergistic effect and individual properties of both Pd and graphene significantly enhanced the catalytic properties of hybrid nanocatalysts. The as-synthesized nanocatalysts HRG@Pd and NDG@Pd effectively catalyzed the reaction of various aryl halides, including chloro-, bromo-, and iodobenzene, with benzene boronic acid in water comprising sodium monododecyl sulfate ( $\text{NaC}_{12}\text{H}_{25}\text{SO}_4$ ) and  $\text{K}_3\text{PO}_4$  under aerobic conditions to obtain biaryls (Figure 9). The turnover number (TON) and turnover frequency (TOF) values for the nanocatalyst were calculated and are graphically illustrated in Figures 10 and 11. It was found that the TON value obtained for NDG@Pd was much higher than that of the Pd nanoparticles. However, it was similar to HRG@Pd. The TOF values of NDG@Pd were found to be higher than the HRG@Pd. TON and TOF values were calculated by using the Equations (1) and (2) [17].

$$\text{Turnover number (TON)} = \frac{\text{Moles of desired product formed}}{\text{Number of active sites}} \quad (1)$$

$$\text{Turnover frequency (TOF)} = \frac{\text{Turnover number}}{\text{Reaction time}} \quad (2)$$



**Figure 9.** Schematic representation of the Suzuki reaction of iodobenzene, bromobenzene, and chlorobenzene with phenylboronic acid under aqueous conditions.

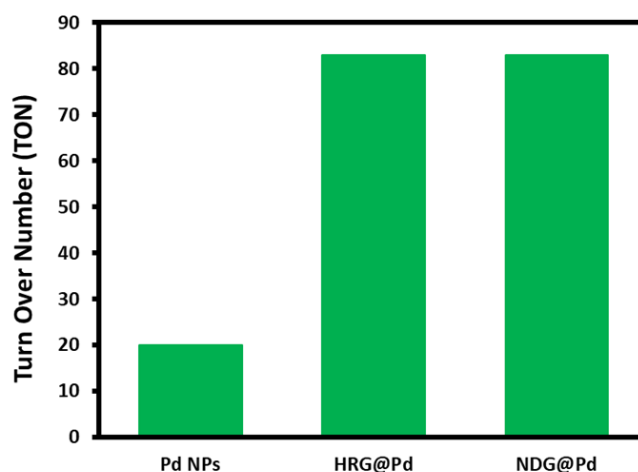


**Figure 10.** Graphical illustration of comparative turnover number (TON) values.

The results found in the present study revealed that iodo- and bromo- substituted aryl halide yielded 100% coupled product at the fastest reaction rate (within 25 min). However, the chloro-substituted aryl halide yielded a ~56% product. A comparison between the catalytic performance of the previously reported nanocatalyst results revealed that iodo-substituted aryl halide yielded a coupled product at the fastest reaction rate (within 30 min) for both of the catalysts: However, the bromo-substituted substrates yielded 100% within 50 min. Chloro-substituted substrates yielded a

~54% product within 60 min [17]. The nanocatalyst of the current study results revealed that the nitrogen-doped graphene-based palladium catalyst was an excellent catalyst for Suzuki–Miyaura coupling compared to our previously reported nanocomposite catalyst [17]. The kinetics of the reaction were examined using gas chromatography (GC), studied by collecting the reaction mixture at equal intervals of time and by quenching it immediately. A graphical representation of the data is presented in Figures 12 and 13. Although the NDG@Pd had a small specific surface area when compared to the HRG@Pd, it displayed excellent catalytic activity that was relatively high when compared to the later catalyst. The enhanced catalytic activity of NDG@Pd could be attributed to the formation of various active sites and defects due to the doping with N-atoms.

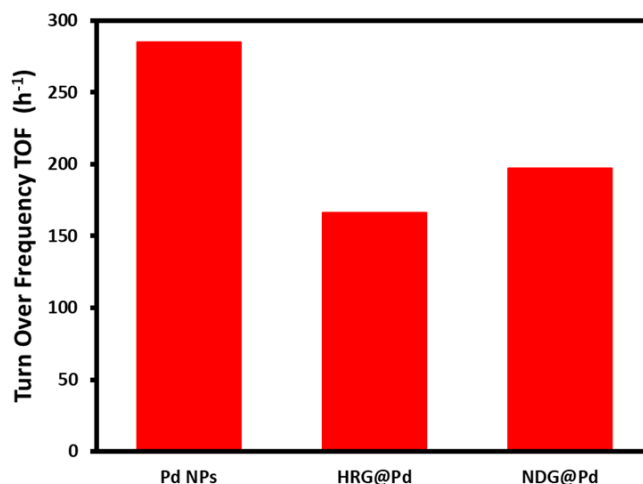


Figure 11. Graphical illustration of comparative turnover frequency (TOF) values.

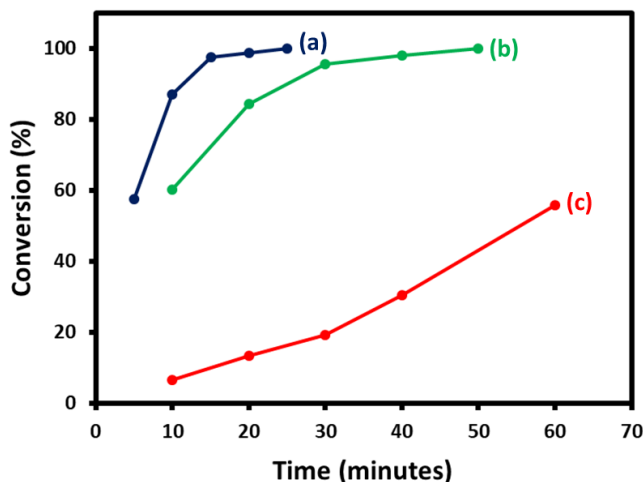
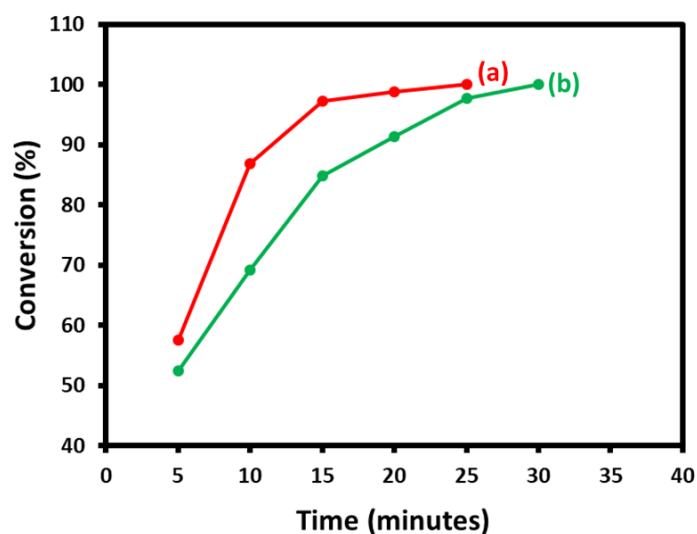
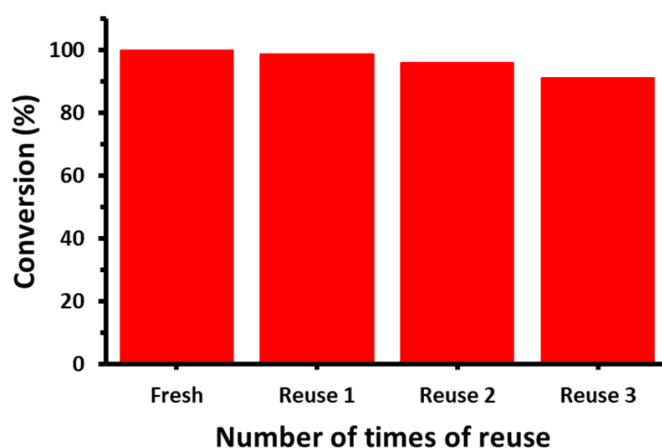


Figure 12. Time-dependent conversion efficiency of the Suzuki reaction employing NDG@Pd for various substrates ((a) iodobenzene, (b) bromobenzene, and (c) chlorobenzene) with phenylboronic acid under aqueous and aerobic conditions (determined by gas chromatography (GC) analysis).

A recyclability study of the prepared nanocatalyst, i.e. NDG@Pd, was carried out in order to check the stability of the catalyst, and it was found that activity marginally reduced upon consequent use. The formation of a Suzuki-coupled product reduced from 100% to 91% after four times of use. In order to ascertain the reason, the reaction mixture was subjected to Inductively coupled plasma mass spectrometry (ICP-MS) analysis. Upon analysis, it was found that the reaction mixture contained 69 ppb of Pd metal, which indicated that there was a minuscule leaching of Pd metal, which could have been the reason for the slender depreciation in the catalytic performance. A graphical illustration of the results obtained is given in Figure 14.



**Figure 13.** Comparison study of time-dependent conversion efficiency of the Suzuki reaction employing (a) NDG@Pd and (b) HRG@Pd nanocatalysts for iodobenzene with phenylboronic acid under aqueous and aerobic conditions (determined by GC analysis).



**Figure 14.** Graphical representation of the conversion product obtained by the reuse of the catalyst for the catalytic conversion of iodobenzene.

### 3. Materials and Methods

#### 3.1. Materials

Natural graphite powder (99.999%, 200 mesh) was purchased from Alfa Aesar (Tewksbury, MA, USA). Palladium (II) chloride ( $\text{PdCl}_2$  99.99%), ammonia hydroxide solution ( $\text{NH}_4\text{OH}$ ), hydrazine hydrate ( $\text{N}_2\text{H}_4$ ), concentrated sulfuric acid ( $\text{H}_2\text{SO}_4$  98%), potassium permanganate ( $\text{KMnO}_4$  99%), sodium nitrate ( $\text{NaNO}_3$ , 99%), hydrogen peroxide ( $\text{H}_2\text{O}_2$ , 30 wt %), chlorobenzene (99.5%), iodobenzene (99%), bromobenzene (99.5%), sodium dodecyl sulfate (98%), phenyl boronic acid (95%), tripotassium phosphate (98%), all organic solvents, and deuterated solvents for NMR studies were obtained from Aldrich Chemicals (St. Louis, MI, USA) and were used directly without further purification.

#### 3.2. Methods

##### 3.2.1. Preparation of Graphene Oxide (GRO)

Graphite oxide (GO) was synthesized from graphite powder using a previously reported modified Hummers method [41,42]. Briefly, a mixture of 0.5 g of graphite powder and 0.5 g of  $\text{NaNO}_3$  in 23 mL of  $\text{H}_2\text{SO}_4$  was stirred for 10 min in an ice bath in a 100-mL flask. Thereafter, 3 g of  $\text{KMnO}_4$  was slowly

added to this mixture until the color of the mixture was changed to dark green. The mixture was allowed to stir thoroughly for several minutes. After this, the ice bath was removed, and the mixture was placed in a water bath and slightly heated to 35 to 40 °C. Stirring continued for another 1 h, which resulted in the formation of thick paste. Subsequently, deionized water (DI) (40 mL) was added to the mixture, and stirring continued at ~90 °C for another half of an hour. After 30 min, at the same temperature, more DI water (100 mL) was added to the mixture, and subsequently 3 mL of H<sub>2</sub>O<sub>2</sub> was also added. This resulted in an immediate change in the color of the mixture from dark brown to light yellow. After cooling, the mixture was filtered and washed several times (3 times using 100 mL of water each time). After washing, a thick brown paste was obtained, which was dispersed in DI water (100 mL) and subjected to a centrifuge for a short time (~2–3 min) at a low speed of 1000 rpm. Similarly, this step was repeated around 4–5 times, using the same amount of water, until all of the floating particles were removed. Finally, the as-obtained mixture was dispersed again in 100 mL of DI water and was centrifuged at a high speed of 8000 rpm to remove any remaining small pieces of GO. After this, the resultant paste was redispersed in water via mild sonication to obtain a solution of GRO.

### 3.2.2. Preparation of N-Doped Graphene-Palladium nanocatalyst (NDG@Pd)

In a typical procedure, the as-synthesized graphite oxide (200 mg) was dispersed in 40 mL of distilled water and was sonicated for 30 min to obtain graphene oxide (GRO) sheets. The resulting suspension was taken in a round bottom flask, to which 100 mg (0.563 mmol) of PdCl<sub>2</sub>, 4 mL of NH<sub>4</sub>OH, and 4 mL of hydrazine hydrate were added simultaneously. The reaction flask was equipped with a condenser, and the dispersion was allowed to stir for 3 h at 90 °C in a water bath. After 3 h of stirring, the reaction mixture was allowed to cool down, and then the solid black precipitate was collected and filtered. The as-obtained sample was further washed with DI water several times to remove excess hydrazine hydrate residue and was redispersed in water via sonication. This suspension was centrifuged at 4000 rpm for another 30 min. The final product was collected by simple decantation and dried under a vacuum at 40 °C. A highly reduced graphene oxide (HRG) and Pd nanocatalyst (HRG@Pd) was also prepared in a similar fashion without adding ammonium hydroxide to the reaction mixture.

### 3.2.3. Catalytic Activity

In a typical experiment, a mixture of sodium dodecyl sulfate (144 mg, 0.5 mmol), tripotassium phosphate (K<sub>3</sub>PO<sub>4</sub>, 399 mg), phenylboronic acid (146 mg, 1.2 mmol), and deionized water (20 mL) was taken in a 100-mL round bottom flask. Halobenzene (1.0 mmol) was added to this mixture under stirring, followed by the as-prepared NDG@Pd and/or HRG@Pd nanocatalyst (5 mol %, 5.32 mg). The mixture was stirred at 100 °C in an oil bath for 5 min and then extracted with ethyl acetate (3 × 20 mL). The combined organic extract was dried over anhydrous sodium sulfate (Na<sub>2</sub>SO<sub>4</sub>), and the resulting mixture was analyzed by gas chromatography (GC). In order to identify the product obtained from the catalytic reaction, the as-obtained mixture was crystallized from ethanol. The resulting product was characterized using <sup>1</sup>H and <sup>13</sup>C solution Nuclear magnetic resonance spectroscopy (NMR) and mass spectroscopy. <sup>1</sup>H-NMR δ = 8.25 (d, *J* = 8.3 Hz, 4H, C–CH, next to ipso), 7.25–7.26 (m, 6H, remaining protons of phenyl ring); <sup>13</sup>C-NMR 141.3 (2C, C–C, ipso), 128.8 (4C, CH–CH), 127.3 (2C, CH–CH, edge carbons), 127.2 (4C, C–CH, next to ipso); electron impact mass spectrometry (EIMS) *m/z* 154 (M<sup>+</sup>). In order to check the reusability of the catalysts, the residual catalyst was collected by centrifugation after the reaction. The catalyst was washed several times with water to remove any remaining contaminants. The reusability reactions were performed in a similar fashion to the aforementioned procedure using iodobenzene as the main reactant.

### 3.2.4. Characterization

The as-synthesized NDG@Pd nanocatalyst and the product obtained from the Suzuki reactions were characterized by UV–Vis spectroscopy (Perkin Elmer lambda 35 (Waltham, MA, USA)),

high-resolution transmission electron microscopy (HRTEM), Energy-dispersive X-ray spectroscopy (EDX) (JEM 2100F (JEOL, Tokyo, Japan)), FT-IR spectroscopy (Perkin Elmer, 1000 FT-IR spectrometer, Waltham, MA, USA), BET surface area (NOVA 4200e surface area & pore size analyzer (Quantachrome Instruments, FL, USA)), nuclear magnetic resonance spectroscopy (NMR) (JEOL ECP-400 spectrometer, Tokyo, Japan), and gas chromatography (GC) (GC 7890A, Agilent Technologies Inc., Santa Clara, CA, USA, equipped with a flame ionization detector (FID) and a 19019S-001 HPPONA column, Santa Clara, CA, USA). All of the NMR samples were prepared in CDCl<sub>3</sub> with tetramethylsilane (TMS) as an internal standard. The XRD analysis of the as-prepared nanocatalyst was carried out using a D2 Phaser X-ray diffractometer (Bruker, Germany) and Cu K $\alpha$  radiation ( $k = 1.5418 \text{ \AA}$ ). XPS spectra were measured on a PHI 5600 Multi-Technique XPS (Physical Electronics, Lake Drive East, Chanhassen, MN, USA) using monochromatized Al K $\alpha$  at 1486.6 eV. Peak fitting was performed using CASA XPS Version 2.3.14 software, USA.

#### 4. Conclusions

In summary, we developed a one-pot method for the preparation of NDG@Pd nanocatalysts and also studied their catalytic activity in Suzuki–Miyaura coupling reactions. This novel nitrogen-doped graphene-based palladium catalyst was prepared by using NH<sub>4</sub>OH and hydrazine hydrate as doping and reducing agents. The resultant nanocatalyst showed a homogeneous distribution of Pd NPs on the surface of NDG with excellent dispersion properties. The as-prepared NDG@Pd nanocatalyst was used as an effective catalyst for various Suzuki–Miyaura coupling reactions in aqueous solution. Furthermore, when the catalytic activity of NDG@Pd was compared to HRG@Pd in the coupling reactions, it was revealed that the N-doped catalysts displayed enhanced activity due to the presence of more active sites and defects on the surface of the catalyst. This was because nitrogen doping has facilitated the formation of defects in the catalysts, which may have acted as active sites during the reaction. Furthermore, the results also suggested that the surface area of the catalyst increased due to nitrogen doping. Due to this, the catalytic activity of the catalyst was enhanced. These features, together with the ease of the synthetic process, may promote the suitability of the method for large-scale production of efficient heteroatom-doped catalysts for various important organic transformations, including Suzuki–Miyaura couplings.

**Supplementary Materials:** The following are available online at <http://www.mdpi.com/2073-4344/9/5/469/s1>, Figure S1: XRD diffractogram of nitrogen doped graphene based palladium fresh nanocatalyst (NDG@Pd) (green line) and nitrogen doped graphene based palladium used nanocatalyst (NDG@Pd) (red line).

**Author Contributions:** J.V.S.K., S.F.A., and M.K. (Mujeeb Khan) designed the project. M.K. (Mufsir Kuniyil), S.F.A., M.K. (Mujeeb Khan), and M.R.S. helped to draft the manuscript. M.K. (Mufsir Kuniyil), M.E.A., and M.R.S. carried out the experimental part and characterization analysis. J.V.S.K., S.F.A., A.A.-W., and M.R.H.S. provided scientific guidance for successful completion of the project and also helped to draft the manuscript. All authors read and approved the final manuscript.

**Funding:** “This research was funded by Deanship of Scientific Research, King Saud University. Research group project No. RG-1436-032” and “The APC was funded by Deanship of Scientific Research, King Saud University. Research group project No. RG-1436-032”.

**Acknowledgments:** The authors extend their appreciation to the Deanship of Scientific Research at King Saud University for funding this work through the research group project No. RG-1436-032.

**Conflicts of Interest:** The authors declare that they have no conflicts of interest.

#### References

1. Rao, C.; Sood, A.; Subrahmanyam, K.; Govindaraj, A. Graphene: the new two-dimensional nanomaterial. *Angew. Chem. Int. Ed.* **2009**, *48*, 7752–7777. [[CrossRef](#)] [[PubMed](#)]
2. Geim, A.K.; Novoselov, K.S. The rise of graphene. In *Nanoscience and Technology: A Collection of Reviews from Nature Journals*; World Scientific: Singapore, 2010; pp. 11–19.
3. Huang, X.; Yin, Z.; Wu, S.; Qi, X.; He, Q.; Zhang, Q.; Yan, Q.; Boey, F.; Zhang, H. Graphene-based materials: synthesis, characterization, properties, and applications. *small* **2011**, *7*, 1876–1902. [[CrossRef](#)] [[PubMed](#)]

4. Wan, X.; Huang, Y.; Chen, Y. Focusing on energy and optoelectronic applications: a journey for graphene and graphene oxide at large scale. *Acc. Chem. Res.* **2012**, *45*, 598–607. [[CrossRef](#)]
5. Denk, R.; Hohage, M.; Zeppenfeld, P.; Cai, J.; Pignedoli, C.A.; Söde, H.; Fasel, R.; Feng, X.; Müllen, K.; Wang, S. Exciton-dominated optical response of ultra-narrow graphene nanoribbons. *Nat. Commun.* **2014**, *5*. [[CrossRef](#)]
6. Assal, M.E.; Shaik, M.R.; Kuniyil, M.; Khan, M.; Al-Warthan, A.; Siddiqui, M.R.H.; Khan, S.M.; Tremel, W.; Tahir, M.N.; Adil, S.F. A highly reduced graphene oxide/ZrO<sub>x</sub>-MnCO<sub>3</sub> or-Mn<sub>2</sub>O<sub>3</sub> nanocomposite as an efficient catalyst for selective aerial oxidation of benzylic alcohols. *RSC Adv.* **2017**, *7*, 55336–55349. [[CrossRef](#)]
7. Gao, N.; Fang, X. Synthesis and development of graphene–inorganic semiconductor nanocomposites. *Chem. Rev.* **2015**, *115*, 8294–8343. [[CrossRef](#)] [[PubMed](#)]
8. Yin, P.T.; Shah, S.; Chhowalla, M.; Lee, K.-B. Design, synthesis, and characterization of graphene–nanoparticle hybrid materials for bioapplications. *Chem. Rev.* **2015**, *115*, 2483–2531. [[CrossRef](#)] [[PubMed](#)]
9. Chng, L.L.; Erathodiyil, N.; Ying, J.Y. Nanostructured catalysts for organic transformations. *Acc. Chem. Res.* **2013**, *46*, 1825–1837. [[CrossRef](#)]
10. Alonso, D.; Baeza, A.; Chinchilla, R.; Gómez, C.; Guillena, G.; Pastor, I.; Ramón, D. Solid-Supported Palladium Catalysts in Sonogashira Reactions: Recent Developments. *Catalysts* **2018**, *8*, 202. [[CrossRef](#)]
11. Hervé, G.; Sartori, G.; Enderlin, G.; Mackenzie, G.; Len, C. Palladium-catalyzed Suzuki reaction in aqueous solvents applied to unprotected nucleosides and nucleotides. *RSC Adv.* **2014**, *4*, 18558–18594. [[CrossRef](#)]
12. Len, C.; Bruniaux, S.; Delbecq, F.; Parmar, V.S. Palladium-Catalyzed Suzuki–Miyaura Cross-Coupling in Continuous Flow. *Catalysts* **2017**, *7*, 146. [[CrossRef](#)]
13. Maluenda, I.; Navarro, O. Recent developments in the Suzuki–Miyaura reaction: 2010–2014. *Molecules* **2015**, *20*, 7528–7557. [[CrossRef](#)]
14. Han, F.-S. Transition-metal-catalyzed Suzuki–Miyaura cross-coupling reactions: a remarkable advance from palladium to nickel catalysts. *Chem. Soc. Rev.* **2013**, *42*, 5270–5298. [[CrossRef](#)] [[PubMed](#)]
15. Erami, R.; Díaz-García, D.; Prashar, S.; Rodríguez-Diéguez, A.; Fajardo, M.; Amirnasr, M.; Gómez-Ruiz, S. Suzuki–Miyaura CC Coupling Reactions Catalyzed by Supported Pd Nanoparticles for the Preparation of Fluorinated Biphenyl Derivatives. *Catalysts* **2017**, *7*, 76. [[CrossRef](#)]
16. Nasrollahzadeh, M.; Issaabadi, Z.; Tohidi, M.M.; Mohammad Sajadi, S. Recent progress in application of graphene supported metal nanoparticles in C–C and C–X coupling reactions. *The Chemical Record* **2018**, *18*, 165–229. [[CrossRef](#)]
17. Khan, M.; Kuniyil, M.; Shaik, M.R.; Khan, M.; Adil, S.F.; Al-Warthan, A.; Alkathlan, H.Z.; Tremel, W.; Tahir, M.N.; Siddiqui, M.R.H. Plant Extract Mediated Eco-Friendly Synthesis of Pd@ Graphene Nanocatalyst: An Efficient and Reusable Catalyst for the Suzuki–Miyaura Coupling. *Catalysts* **2017**, *7*, 20. [[CrossRef](#)]
18. Wang, J.; Gu, H. Novel metal nanomaterials and their catalytic applications. *Molecules* **2015**, *20*, 17070–17092. [[CrossRef](#)]
19. Kuila, T.; Bose, S.; Mishra, A.K.; Khanra, P.; Kim, N.H.; Lee, J.H. Chemical functionalization of graphene and its applications. *Prog. Mater. Sci.* **2012**, *57*, 1061–1105. [[CrossRef](#)]
20. Vinayan, B.; Sethupathi, K.; Ramaprabhu, S. Facile synthesis of triangular shaped palladium nanoparticles decorated nitrogen doped graphene and their catalytic study for renewable energy applications. *Int. J. Hydrogen Energy* **2013**, *38*, 2240–2250. [[CrossRef](#)]
21. Kabir, S.; Artyushkova, K.; Serov, A.; Atanassov, P. Role of Nitrogen Moieties in N-Doped 3D-Graphene Nanosheets for Oxygen Electroreduction in Acidic and Alkaline Media. *ACS Appl. Mater. Interfaces* **2018**, *10*, 11623–11632. [[CrossRef](#)]
22. Zhou, Y.; Neyerlin, K.; Olson, T.S.; Pylypenko, S.; Bult, J.; Dinh, H.N.; Gennett, T.; Shao, Z.; O’Hayre, R. Enhancement of Pt and Pt-alloy fuel cell catalyst activity and durability via nitrogen-modified carbon supports. *Energy Environ. Sci.* **2010**, *3*, 1437–1446. [[CrossRef](#)]
23. Geng, D.; Chen, Y.; Chen, Y.; Li, Y.; Li, R.; Sun, X.; Ye, S.; Knights, S. High oxygen-reduction activity and durability of nitrogen-doped graphene. *Energy Environ. Sci.* **2011**, *4*, 760–764. [[CrossRef](#)]
24. Qiao, X.; Liao, S.; You, C.; Chen, R. Phosphorus and nitrogen dual doped and simultaneously reduced graphene oxide with high surface area as efficient metal-free electrocatalyst for oxygen reduction. *Catalysts* **2015**, *5*, 981–991. [[CrossRef](#)]
25. Zheng, Y.; Jiao, Y.; Zhu, Y.; Li, L.H.; Han, Y.; Chen, Y.; Du, A.; Jaroniec, M.; Qiao, S.Z. Hydrogen evolution by a metal-free electrocatalyst. *Nat. Commun.* **2014**, *5*, 3783. [[CrossRef](#)]

26. Jeon, I.Y.; Zhang, S.; Zhang, L.; Choi, H.J.; Seo, J.M.; Xia, Z.; Dai, L.; Baek, J.B. Edge-selectively sulfurized graphene nanoplatelets as efficient metal-free electrocatalysts for oxygen reduction reaction: the electron spin effect. *Adv. Mater.* **2013**, *25*, 6138–6145. [[CrossRef](#)]
27. Sheng, Z.-H.; Shao, L.; Chen, J.-J.; Bao, W.-J.; Wang, F.-B.; Xia, X.-H. Catalyst-free synthesis of nitrogen-doped graphene via thermal annealing graphite oxide with melamine and its excellent electrocatalysis. *ACS nano* **2011**, *5*, 4350–4358. [[CrossRef](#)]
28. Jiang, B.; Song, S.; Wang, J.; Xie, Y.; Chu, W.; Li, H.; Xu, H.; Tian, C.; Fu, H. Nitrogen-doped graphene supported Pd@PdO core-shell clusters for CC coupling reactions. *Nano Res.* **2014**, *7*, 1280–1290. [[CrossRef](#)]
29. Khan, M.; Al-Marri, A.H.; Khan, M.; Shaik, M.R.; Mohri, N.; Adil, S.F.; Kuniyil, M.; Alkathlan, H.Z.; Al-Warthan, A.; Tremel, W. Green approach for the effective reduction of graphene oxide using salvadora persica l. root (miswak) extract. *Nanoscale Res. Lett.* **2015**, *10*, 281. [[CrossRef](#)]
30. Vinoth, R.; Babu, S.G.; Bahnmann, D.; Neppolian, B. Nitrogen doped reduced graphene oxide hybrid metal free catalyst for effective reduction of 4-nitrophenol. *Sci. Adv. Mater.* **2015**, *7*, 1443–1449. [[CrossRef](#)]
31. Lin, Z.; Waller, G.H.; Liu, Y.; Liu, M.; Wong, C.-p. Simple preparation of nanoporous few-layer nitrogen-doped graphene for use as an efficient electrocatalyst for oxygen reduction and oxygen evolution reactions. *Carbon* **2013**, *53*, 130–136. [[CrossRef](#)]
32. Khan, M.; Khan, M.; Kuniyil, M.; Adil, S.F.; Al-Warthan, A.; Alkathlan, H.Z.; Tremel, W.; Tahir, M.N.; Siddiqui, M.R.H. Biogenic synthesis of palladium nanoparticles using *Pulicaria glutinosa* extract and their catalytic activity towards the Suzuki coupling reaction. *Dalton Trans.* **2014**, *43*, 9026–9031. [[CrossRef](#)]
33. Duan, X.; O'Donnell, K.; Sun, H.; Wang, Y.; Wang, S. Sulfur and nitrogen co-doped graphene for metal-free catalytic oxidation reactions. *Small* **2015**, *11*, 3036–3044. [[CrossRef](#)]
34. Cui, L.; Chen, X.; Liu, B.; Chen, K.; Chen, Z.; Qi, Y.; Xie, H.; Zhou, F.; Rummeli, M.H.; Zhang, Y.; et al. Highly Conductive Nitrogen-Doped Graphene Grown on Glass toward Electrochromic Applications. *ACS Appl. Mater. Interfaces* **2018**, *10*, 32622–32630. [[CrossRef](#)]
35. Zhang, W.; Huang, H.; Li, F.; Deng, K.; Wang, X. Palladium nanoparticles supported on graphitic carbon nitride-modified reduced graphene oxide as highly efficient catalysts for formic acid and methanol electrooxidation. *J. Mater. Chem.:A* **2014**, *2*, 19084–19094. [[CrossRef](#)]
36. Wang, X.; Hou, Z.; Ikeda, T.; Oshima, M.; Kakimoto, M.-A.; Terakura, K. Theoretical Characterization of X-ray Absorption, Emission, and Photoelectron Spectra of Nitrogen Doped along Graphene Edges. *J. Phys. Chem. A* **2013**, *117*, 579–589. [[CrossRef](#)] [[PubMed](#)]
37. Yousaf, A.B.; Imran, M.; Farooq, M.; Kasak, P. Interfacial Phenomenon and Nanostructural Enhancements in Palladium Loaded Lanthanum Hydroxide Nanorods for Heterogeneous Catalytic Applications. *Sci. Rep.* **2018**, *8*, 4354. [[CrossRef](#)]
38. Chen, X.; Chen, B. Macroscopic and Spectroscopic Investigations of the Adsorption of Nitroaromatic Compounds on Graphene Oxide, Reduced Graphene Oxide, and Graphene Nanosheets. *Environ. Sci. Technol.* **2015**, *49*, 6181–6189. [[CrossRef](#)]
39. Babaei, A.; Jiang, S.P.; Li, J. Electrocatalytic Promotion of Palladium Nanoparticles on Hydrogen Oxidation on Ni/GDC Anodes of SOFCs via Spillover. *J. Electrochem. Soc.* **2009**, *156*, B1022–B1029. [[CrossRef](#)]
40. Mpungose, P.P.; Vundla, Z.P.; Maguire, G.E.M.; Friedrich, H.B. The Current Status of Heterogeneous Palladium Catalysed Heck and Suzuki Cross-Coupling Reactions. *Molecules* **2018**, *23*, 1676. [[CrossRef](#)]
41. Hummers Jr, W.S.; Offeman, R.E. Preparation of Graphitic Oxide. *J. Am. Chem. Soc.* **1958**, *80*, 1339. [[CrossRef](#)]
42. Cote, L.J.; Kim, F.; Huang, J. Langmuir–Blodgett assembly of graphite oxide single layers. *J. Am. Chem. Soc.* **2008**, *131*, 1043–1049. [[CrossRef](#)] [[PubMed](#)]

